Preprints of the 21st IFAC World Congress (Virtual)
Berlin, Germany, July 12-17, 2020

Decentralized Multivariable Vector Current Control of Grid-connected Voltage Source Inverters

Mahdieh S. Sadabadi * **Qobad Shafiee** **

* *Department of Automatic Control and Systems Engineering, University of Sheffield, Sheffield, United Kingdom (e-mail: m.sadabadi@sheffield.ac.uk).*
** *Department of Electrical Engineering, University of Kurdistan, Sanandaj, Kurdistan, Iran (email: q.shafiee@uok.ac.ir).*

Abstract: Increasing the number of grid-connected inverters in power systems imposes several challenges. One of the main challenges is the complexity and uncertainty of the dynamical model of the inverters due to the large numbers of grid-connected inverters and disconnection of inverters. To address this challenge, we present a scalable direct-quadrature current control strategy for parallel voltage source inverters in a rotating reference frame. The control structure is based on a decentralized multivariable proportional integral (PI) current control mechanism and provides stability and zero steady-state errors. The proposed control approach has the main advantages of flexibility, allowing disconnection/connection of inverters on the basis of the required power level. The effectiveness of the proposed vector current control strategy is evaluated through simulation case studies in MATLAB/Simscape Electrical.

Keywords: Vector current control, Lyapunov theory, Scalable control design, Parallel voltage sources inverters, Rotating reference frame, Decentralized control, Grid-connected voltage source inverters.

1. INTRODUCTION

Renewable energy sources are commonly interfaced to the grid through voltage source inverters (VSIs) with passive output filters. The duty of the filters is to mitigate the current harmonic contents injected by the inverters. One of the common control problems in the grid-connected VSIs is about the design of a current controller scheme (Sadabadi et al. (Oct. 2017)).

The most widely used current control approach for VSIs is vector current control that is based on the control of two independent d-axis and q-axis current components in a Synchronous Reference Frame (SFR), while the synchronization is done via a phase-locked loop (PLL) (Svensson (May 2001)). This type of control approaches basically involves a transformation from three-phase steady state into the d-q axis in order to control active and reactive power separately (Hannan et al. (December 2018)).

The vector current control approaches for VSIs with L-type filters usually utilize conventional Proportional-Integral (PI) controllers (e.g. Schauder and Mehta (1993)) or modified PIs (e.g. Bahrani et al. (July 2011,A)) whose duty is to compensate for the only dominant pole of each axis by the zero of the PI controllers.

The problem of the current control of VSIs becomes challenging when multiple VSIs are connected to the same grid. In this case, there are interactions among different VSIs. To deal with this case, a typical strategy is to assume that each inverter is decoupled from others and the control schemes are designed based on the single-inverter model and without considering the interaction terms. This strategy only works for stiff AC grids as the interactions among different inverters are not significant and each VSI can be independently controlled. However, in weak AC power grids with high grid impedances, interactions among inverters cannot be ignored. Neglecting the interaction terms results in instability and/or poor performance of the system. Therefore, the impact of the interactions among inverters and their influence on the overall stability are important. Moreover, as the number of VSIs connected to the power grid is increasing, a new VSI tied to the grid impacts the overall AC network characteristics and the operation of other VSIs (Bayo-Salas et al. (2016)). Disconnection of VSIs from the AC network influences the system stability and performance. A change in the architecture of the AC grid might reduce the overall stability as well as the desired performance specifications of the system. Therefore, the current controllers of VSIs must be appropriately designed such that they guarantee stability under uncertainty in the grid configuration.

To the best of authors's knowledge, the literature is mainly limited to single-inverter systems and only few references are devoted to parallel grid-tied inverters. A stability analysis of control interactions in a two-parallel-VSI system has been carried out in Bayo-Salas et al. (2016). A control approach for an AC grid-based multi-infeed VSI has been proposed in Li et al. (2010). A frequency-domain current control approach for parallel grid-connected inverters has been presented in Kammer et al. (Jul. 2019). A main drawback of these methods is that the control design is based on the global model of the system. Therefore, these control approaches cannot guarantee the stability of the whole grid if there is a change in the grid configuration (e.g. due to the disconnection of an inverter).

The main objective of this paper is to investigate and develop a new systematic control strategy for the parallel grid-connected VSIs. More specifically, we are interested in the design of decentralized multivariable PI controllers, which are the most well-known and easy-to-implement regulators, in the synchronous reference frame (dq frame). The current control design is based on a scalable approach, where the design of

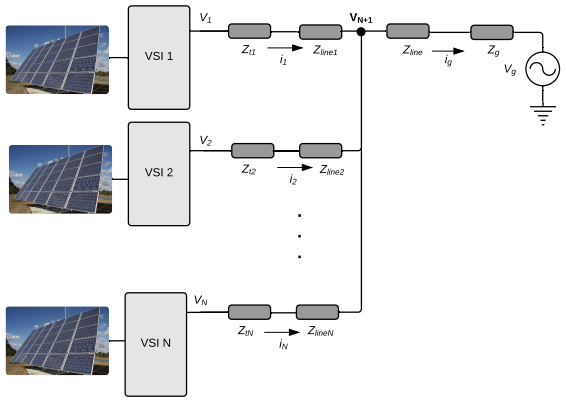

Fig. 1. Schematic diagram of N-parallel grid-tied voltage source inverters.

each current controller is independent of the interconnection of other inverters to the grid. The PI control design problem is formulated as a linear matrix inequality (LMI) which is always feasible. Each VSI has its own controller in order to control its own inverter side current and there is no coupling among the other current controllers. The proposed approach is applicable to both single-phase and three-phase systems. The scalability of the design and asymptotic stability of the parallel grid-connected VSIs are ensured by utilizing a Lyapunov-based framework with a separable quadratic-type structured Lyapunov function as well as the LaSalle's invariance principle. The proposed control approach has the main advantages of flexibility, allowing disconnection/connection of VSIs on the basis of the required power level. The efficiency of the proposed current control strategy is evaluated via simulation case studies carried out in MATLAB/Simscape Electrical.

The rest of the paper is organized as follows: A dynamical model of parallel grid-tied inverters is presented in Section 2. Section 3 proposes a decentralized multivariable PI-based current control framework. The scalable control design strategy is presented in Section 4. Simulation case studies are given in Section 5. Finally, Section 6 concludes the paper.

Throughout the paper, matrices I_n and $0_{m\times n}$ are the identity matrix of dimensions $n\times n$ and the zero matrix of dimension $m\times n$, respectively. The symbols A^T and $\star$ indicate the transpose of matrix A and symmetric blocks in block matrices, respectively. For symmetric matrices, $P>0$ ($P\geq 0$) shows that matrix P is positive-definite (positive semidefinite), whereas $P<0$ ($P\leq 0$) indicates that P is a negative-definite (negative semidefinite) matrix.

2. DYNAMICAL MODEL

This section presents a mathematical model of three-phase parallel grid-tied voltage source inverters with L filters, as shown in Fig. 1. In this figure, $Z_{t_i}=R_{t_i}+j\omega_0 L_{t_i}$, $Z_g=r_g+j\omega_0 L_g$, and $Z_{line_i}=r_{line_i}+j\omega_0 L_{line_i}$ respectively are inverter impedance, grid impedance, and line impedance. The angular frequency of the system is $\omega_0=2\pi f_0$, where f_0 is the nominal frequency. The dynamics of each inverter are mathematically described as follows:

$$\frac{di_i}{dt}=-\frac{R_i}{L_i}i_i+\frac{1}{L_i}V_i-\frac{r_g+R_{line}}{L_i}i_g-\frac{L_g+L_{line}}{L_i}\frac{di_g}{dt}-\frac{1}{L_i}V_g \quad (1)$$

where

$$R_i=R_{t_i}+r_{line_i},\quad L_i=L_{t_i}+L_{line_i} \quad (2)$$

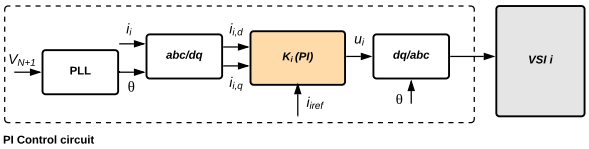

Fig. 2. PI current control circuit of VSI i.

for $i=1,\ldots,N$, where i_i, i_g, V_i, and V_g are the inverter current, the grid current, the terminal voltage of inverter i, and the grid voltage, respectively. The grid current can be expressed as $i_g=\sum_{j=1}^{N} i_j$.

2.1 Interaction Terms in Parallel Grid-tied Inverters

The interaction terms among all N inverters are described as follows:

$$L\begin{bmatrix}\frac{di_1}{dt}\\ \frac{di_2}{dt}\\ \vdots\\ \frac{di_N}{dt}\end{bmatrix}=-R\begin{bmatrix}i_1\\ i_2\\ \vdots\\ i_N\end{bmatrix}+\begin{bmatrix}V_1-V_g\\ V_2-V_g\\ \vdots\\ V_N-V_g\end{bmatrix} \quad (3)$$

where

$$L=\begin{bmatrix}L_1+L_g+L_{line} & L_{line}+L_g & \cdots & L_{line}+L_g\\ L_{line}+L_g & L_2+L_g+L_{line} & \cdots & L_g+L_{line}\\ \vdots & \vdots & \ddots & \vdots\\ L_g+L_{line} & L_g+L_{line} & \cdots & L_N+L_g+L_{line}\end{bmatrix}$$
$$R=\begin{bmatrix}R_1+r_g+R_{line} & R_{line}+r_g & \cdots & R_{line}+r_g\\ R_{line}+r_g & R_2+r_g+R_{line} & \cdots & r_g+R_{line}\\ \vdots & \vdots & \ddots & \vdots\\ r_g+R_{line} & r_g+R_{line} & \cdots & R_N+r_g+R_{line}\end{bmatrix} \quad (4)$$

The interactions between two different inverters depend on the grid impedance. If the grid is stiff, i.e. $L_{line}+L_g\approx 0$ and $R_{line}+r_g\approx 0$, the dynamics of the inverters are decoupled. As a result, in the stiff grids, the problem of current control of N-parallel inverters is equivalent to the current control of N decoupled inverters. However, in a weak grid, the grid impedance provides coupling among inverters. Hence, the interaction terms should be considered in the control design and analysis.

2.2 Mathematical Model of Parallel Grid-tied Inverters in Synchronous Reference Frame

Under balanced conditions, the grid-connected system composed of N parallel inverters in Fig .1 is described in the synchronous reference frame (dq frame) by the following equations:

$$\begin{bmatrix}\frac{di_{i,d}}{dt}\\ \frac{di_{i,q}}{dt}\end{bmatrix}=A_{g_i}\begin{bmatrix}i_{i,d}\\ i_{i,q}\end{bmatrix}+B_{u_i}\begin{bmatrix}V_{i,d}\\ V_{i,q}\end{bmatrix}+B_{g1_i}\begin{bmatrix}i_{g,d}\\ i_{g,q}\end{bmatrix}+B_{g2_i}\begin{bmatrix}\frac{di_{g,d}}{dt}\\ \frac{di_{g,q}}{dt}\end{bmatrix}+B_{w_i}\begin{bmatrix}V_{g,d}\\ V_{g,q}\end{bmatrix}$$
$$y_i(t)=C_{g_i}x_{g_i}(t);\quad i=1,\ldots,N \quad (5)$$

where $y_i=[\,i_{i,d}\;\; i_{i,q}\,]^T$ is the output of the inverter i. The signals $i_{i,d}$, $i_{i,q}$, $i_{g,d}$, $i_{g,q}$, $V_{i,d}$, $V_{i,q}$, $V_{g,d}$, and $V_{g,q}$ are the d and q components of the inverter-side current, the grid current, the VSI terminal voltage, and the grid voltage, respectively. The state space matrices are given as follows:

$$A_{g_i} = \begin{bmatrix} -\frac{R_i}{L_i} & \omega_0 \\ -\omega_0 & -\frac{R_i}{L_i} \end{bmatrix}, \quad B_{g1_i} = \begin{bmatrix} -\frac{r_g+R_{line}}{L_i} & \frac{L_g+L_{line}}{L_i}\omega_0 \\ -\frac{L_g+L_{line}}{L_i}\omega_0 & -\frac{r_g+R_{line}}{L_i} \end{bmatrix}$$
$$B_{g2_i} = \begin{bmatrix} -\frac{L_g+L_{line}}{L_i} & 0 \\ 0 & -\frac{L_g+L_{line}}{L_i} \end{bmatrix}, \quad B_{u_i} = \begin{bmatrix} \frac{1}{L_i} & 0 \\ 0 & \frac{1}{L_i} \end{bmatrix}$$
$$B_{w_i} = -\begin{bmatrix} \frac{1}{L_i} & 0 \\ 0 & \frac{1}{L_i} \end{bmatrix}, \quad C_{g_i} = \begin{bmatrix} 1 & 0 \\ 0 & 1 \end{bmatrix}. \tag{6}$$

3. DECENTRALIZED MULTIVARIABLE PI-BASED CURRENT CONTROL FRAMEWORK

In this section, a decentralized multivariable PI-based *dq* current control strategy for the three-phase multi-parallel grid-tied inverters in Fig. 1 is developed. The proposed control approach aims at the current stabilization of the inverters and ensures that current signal of each inverter tracks a *qd* reference current with zero steady state error.

3.1 Current Control Structure

The control input of the inverter i, $i = 1,\ldots,N$ is structured as follows:

$$\begin{bmatrix} V_{i,d} \\ V_{i,q} \end{bmatrix} = K_{P_i}\left(\begin{bmatrix} i_{i,d} \\ i_{i,q} \end{bmatrix} - \begin{bmatrix} i_{i_{ref},d} \\ i_{i_{ref},q} \end{bmatrix}\right) + K_{I_i}\int\left(-\begin{bmatrix} i_{i,d} \\ i_{i,q} \end{bmatrix} + \begin{bmatrix} i_{i_{ref},d} \\ i_{i_{ref},q} \end{bmatrix}\right)dt \tag{7}$$

where $i_{i_{ref},d}$ and $i_{i_{ref},q}$ respectively are the d and q components of the reference signal of the inverter i. The parameters $K_{P_i} \in \mathbb{R}^{2\times 2}$ and $K_{I_i} \in \mathbb{R}^{2\times 2}$ are the proportional and integral gains of the multivariable PI controllers, respectively. The terms $\int(-i_{i,d}+i_{i_{ref},d})dt$ and $\int(-i_{i,q}+i_{i_{ref},q})dt$ are defined as two new variable $I_{i,d}$ and $I_{i,q}$ with the following dynamics:

$$\begin{bmatrix} \frac{dI_{i,d}}{dt} \\ \frac{dI_{i,q}}{dt} \end{bmatrix} = -\begin{bmatrix} i_{i,d} \\ i_{i,q} \end{bmatrix} + \begin{bmatrix} i_{i_{ref},d} \\ i_{i_{ref},q} \end{bmatrix} \tag{8}$$

The PI-based control circuit of VSI i is shown in Fig. 2. In this figure, an enhanced phase-locked loop (PLL) is used to derive the frequency and phase of the system. The dynamics of the PLL are neglected as the grid under study is assumed not to be very weak (Davari and Mohamed (Feb. 2017)).

3.2 Closed-loop Dynamics of Inverter i

For given $i_{i_{ref},d}$ and $i_{i_{ref},q}$, the equilibrium point of (5)-(8) is given by

$$\begin{aligned} &\bar{i}_{i,d} = i_{i_{ref},d}, \quad \bar{i}_{i,q} = i_{i_{ref},q} \\ &\bar{i}_{g,d} = \sum_{j=1}^{N} i_{j_{ref},d}, \quad \bar{i}_{g,q} = \sum_{j=1}^{N} i_{j_{ref},q} \\ &\bar{V}_{i,d} = R_i i_{i_{ref},d} - \omega_0 i_{i_{ref},q} \\ &\quad + (r_g + R_{line})\bar{i}_{g,d} - (L_g + L_{line})\omega_0 \bar{i}_{g,q} + V_{g,d} \\ &\bar{V}_{i,q} = R_i i_{i_{ref},q} - \omega_0 i_{i_{ref},d} \\ &\quad + (r_g + R_{line})\bar{i}_{g,q} + (L_g + L_{line})\omega_0 \bar{i}_{g,d} + V_{g,q} \\ &\begin{bmatrix} \bar{I}_{i,d} \\ \bar{I}_{i,q} \end{bmatrix} = K_{I_i}^{-1}\begin{bmatrix} \bar{V}_{i,d} \\ \bar{V}_{i,q} \end{bmatrix} \end{aligned} \tag{9}$$

The system dynamics in (5) and (8) can be written as follows:

$$\begin{aligned} \dot{x}_i &= A_i x_i + B_i u_i + B_{1_i}\tilde{i}_g + B_{2_i}\dot{\tilde{i}}_g \\ y_i &= C_i x_i \end{aligned} \tag{10}$$

where

$$\begin{aligned} x_i &= \begin{bmatrix} i_{i,d} - \bar{i}_{i,d} & i_{i,q} - \bar{i}_{i,q} & I_{i,d} - \bar{I}_{i,d} & I_{i,q} - \bar{I}_{i,q} \end{bmatrix}^T \\ u_i &= \begin{bmatrix} V_{i,d} - \bar{V}_{i,d} & V_{i,q} - \bar{V}_{i,q} \end{bmatrix}^T \\ \tilde{i}_g &= \begin{bmatrix} i_{g,d} - \bar{i}_{g,d} & i_{g,q} - \bar{i}_{g,q} \end{bmatrix}^T \\ y_i &= \begin{bmatrix} i_{i,d} - \bar{i}_{i,d} & i_{i,q} - \bar{i}_{i,q} \end{bmatrix}^T \end{aligned} \tag{11}$$

and

$$\begin{aligned} A_i &= \begin{bmatrix} A_{g_i} & 0_{2\times 2} \\ -C_{g_i} & 0_{2\times 2} \end{bmatrix}, \quad B_i = \begin{bmatrix} B_{u_i} \\ 0_{2\times 2} \end{bmatrix}, \quad B_{1_i} = \begin{bmatrix} B_{g1_i} \\ 0_{2\times 2} \end{bmatrix} \\ B_{2_i} &= \begin{bmatrix} B_{g2_i} \\ 0_{2\times 2} \end{bmatrix}, \quad C_i = \begin{bmatrix} C_{g_i} & 0_{2\times 2} \end{bmatrix} \end{aligned} \tag{12}$$

The PI-based control law u_i is presented as follows:

$$u_i = K_i x_i \tag{13}$$

where $K_i = \begin{bmatrix} K_{P_i} & K_{I_i} \end{bmatrix}$. The main objective is to design the proportional and integral gains K_{P_i} and K_{I_i} such that the stability of the closed-loop dynamics given in (10) is guaranteed.

4. PROPOSED CONTROL DESIGN STRATEGY

In this section, a scalable control design solution for the problem of PI-based current stabilization of the parallel voltage source inverters is proposed.

4.1 PI-based Current Stabilization of Parallel VSIs

Consider the following separable quadratic type Lyapunov function for the system in (10) consisting of N inverters.

$$V(\mathbf{x}) = \sum_{i=1}^{N} V_i(x_i) + V_{grid}(\tilde{i}_g) \tag{14}$$

where $\mathbf{x} = \begin{bmatrix} x_1^T & x_2^T & \ldots & x_N^T \end{bmatrix}^T$ and

$$\begin{aligned} V_i(x_i) &= x_i^T P_i x_i \\ V_{grid}(\tilde{i}_g) &= \alpha(L_g + L_{line})\tilde{i}_g^T \tilde{i}_g \end{aligned} \tag{15}$$

where

$$P_i = \text{diag}\left(\alpha L_i I_2, \tilde{P}_i\right) \tag{16}$$

and $\alpha > 0$ and $\tilde{P}_i \in \mathbb{R}^{2\times 2}$ is a positive-definite matrix. We need to show that the time derivative of $V(\mathbf{x})$ along the closed-loop trajectories of the system given in (10) is non-positive. The time derivative of $V_i(x_i)$ and $V_{grid}(\tilde{i}_g)$ are presented as follows:

$$\begin{aligned} \dot{V}_i(x_i) &= x_i^T Q_i x_i + x_i^T P_i B_{1_i}\tilde{i}_g + \tilde{i}_g^T B_{1_i}^T P_i x_i + x_i^T P_i B_{2_i}\dot{\tilde{i}}_g + \dot{\tilde{i}}_g^T B_{2_i}^T P_i x_i \\ \dot{V}_{grid}(\tilde{i}_g) &= \alpha(L_g + L_{line})(\dot{\tilde{i}}_g^T \tilde{i}_g + \tilde{i}_g^T \dot{\tilde{i}}_g) \end{aligned} \tag{17}$$

where

$$Q_i = (A_i + B_i K_i)^T P_i + P_i(A_i + B_i K_i) \tag{18}$$

Due to the structure of the Lyapunov matrix P_i in (16), it can be shown that

$$\sum_{i=1}^{N}(x_i^T P_i B_{2_i}\dot{\tilde{i}} + \dot{\tilde{i}}^T B_{2_i}^T P_i x_i) + \alpha(L_g + L_{line})(\dot{\tilde{i}}_g^T \tilde{i}_g + \tilde{i}_g^T \dot{\tilde{i}}_g) = 0 \tag{19}$$

As a result, $\dot{V}(\mathbf{x})$ can be formulated as follows:

$$\dot{V}(\mathbf{x}) = \sum_{i=1}^{N} x_i^T Q_i x_i + 2\alpha\tilde{i}_g^T \begin{bmatrix} -(r_g + R_{line}) & 0 \\ 0 & -(r_g + R_{line}) \end{bmatrix}\tilde{i}_g \tag{20}$$

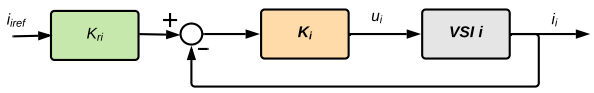

Fig. 3. Block diagram of 2DOF current controller of VSI i.

4.2 Scalable Current Control Design

The time derivative of $V(\mathbf{x})$ in (20) indicates that the asymptotic stability of the overall system with N inverters can be ensured by the stabilization of each inverter via a fixed-structure Lyapunov matrix P_i in (16). The stabilization of VSI i is based on the design of the PI controller K_i such that

$$Q_i = (A_i + B_i K_i)^T P_i + P_i (A_i + B_i K_i) \leq 0 \tag{21}$$

The negative semi-definiteness of Q_i is equivalent to the negative semi-definiteness of matrix $\tilde{Q}_i = P_i^{-1} Q_i P_i^{-1}$ presented as follows:

$$\tilde{Q}_i = Y_i A_i^T + A_i Y_i + B_i G_i + G_i^T B_i^T \tag{22}$$

where $Y_i = P_i^{-1}$ and $G_i = K_i P_i^{-1}$ are parametrized as follows:

$$Y_i = \begin{bmatrix} \alpha^{-1} L_i^{-1} & 0 & 0 & 0 \\ 0 & \alpha^{-1} L_i^{-1} & 0 & 0 \\ 0 & 0 & y_{33_i} & y_{34_i} \\ 0 & 0 & y_{34_i} & y_{44_i} \end{bmatrix} \tag{23}$$

$$G_i = \begin{bmatrix} g_{11_i} & g_{12_i} & g_{13_i} & g_{14_i} \\ g_{21_i} & g_{22_i} & g_{23_i} & g_{24_i} \end{bmatrix} \tag{24}$$

By replacing Y_i and Q_i from (23) and (24) in (22), $\tilde{Q}_i$ is rewritten as follows:

$$\tilde{Q}_i = \begin{bmatrix} \frac{-2R_i}{\alpha L_i^2} + \frac{2g_{11_i}}{L_i} & \frac{1}{L_i}(g_{12_i} + g_{21_i}) & \frac{-1}{\alpha L_i} + \frac{g_{13_i}}{L_i} & \frac{g_{14_i}}{L_i} \\ \star & \frac{-2R_i}{\alpha L_i^2} + \frac{2g_{22_i}}{L_i} & \frac{g_{23_i}}{L_i} & \frac{-1}{\alpha L_i} + \frac{g_{24_i}}{L_i} \\ \star & \star & 0 & 0 \\ \star & \star & \star & 0 \end{bmatrix} \tag{25}$$

The non-positiveness of $\tilde{Q}_i$ implies that the third and fourth columns and rows of $\tilde{Q}_i$ must be equal to zero. As a result,

$$g_{14_i} = 0, \quad g_{23_i} = 0, \quad g_{13_i} = \frac{1}{\alpha}, \quad g_{24_i} = \frac{1}{\alpha} \tag{26}$$

We can show that under the following constraints on g_{11_i}, g_{12_i}, g_{21_i}, and g_{22_i}, the first 2×2 block of $\tilde{Q}_i$ is negative-definite. The negative semi-definiteness of $\tilde{Q}_i$ implies that $Q_i \leq 0$.

$$\begin{gathered} g_{11_i} < \frac{R_i}{\alpha L_i}, \quad g_{22_i} < \frac{R_i}{\alpha L_i} \\ (g_{12_i} + g_{21_i})^2 < 4\left(\frac{-R_i}{\alpha L_i} + g_{11_i}\right)\left(\frac{-R_i}{\alpha L_i} + g_{22_i}\right) \end{gathered} \tag{27}$$

Considering the above conditions on g_i, $\tilde{Q}_i \leq 0$. As a result, the following inequality is feasible, meaning that there always exists a solution G_i constrained as (26)-(27) and $Y_i > 0$ satisfying the following linear matrix inequality (LMI).

$$Y_i A_i^T + A_i Y_i + B_i G_i + G_i^T B_i^T \leq 0 \tag{28}$$

4.3 Asymptotic Stability of Parallel Voltage Source Inverters

In Subsection 4.2, it has been shown that $Q_i \leq 0$. Therefore, $\dot{V}(\mathbf{x}) \leq 0$ for all $\mathbf{x}$. We use the LaSalle's invariance principle (Khalil (2006)) to show that the closed-loop system of N VSIs with the proposed PI control law is asymptotically stable. To this end, we need to show that the only solution of $\dot{V}(\mathbf{x}) = 0$ is $\mathbf{x}(t) = 0$, $\forall t > 0$. To see this, note that $\dot{V}(\mathbf{x}) = 0$ implies that

$$\begin{gathered} \alpha \tilde{i}_g^T \begin{bmatrix} -(r_g + R_{line}) & (L_g + L_{line})\omega_o \\ -(L_g + L_{line})\omega_o & -(r_g + R_{line}) \end{bmatrix} \tilde{i}_g = 0 \Rightarrow \tilde{i}_g = 0, \\ \tilde{x}_i^T Q_i \tilde{x}_i = 0, \end{gathered} \tag{29}$$

for $i = 1\ldots,N$. It is required to show that the only state trajectory of the system that satisfies all the constraints in (29) is origin. Let's compute the set χ as follows:

$$\chi = \underbrace{\{\tilde{i}_g = 0\}}_{\chi_1} \cap \underbrace{\{\tilde{x}_i : \tilde{x}_i^T Q_i \tilde{x}_i = 0\}}_{\chi_2} \tag{30}$$

The trajectories in the set χ_1 are as follows:

$$\tilde{i}_g = 0 \Rightarrow \sum_{j=1}^{N} i_{j,d} = 0 \quad \& \quad \sum_{j=1}^{N} i_{j,q} = 0 \tag{31}$$

Moreover, the set χ_2 implies that there is a state trajectory $x_i^\star$ that maximizes $x_i^T Q_i x_i$, where the maximum value is zero. As a result, $x_i^\star$ satisfies the following equation:

$$\left.\frac{d(x_i^T Q_i x_i)}{dx_i}\right|_{x_i^\star} = 2Q_i x_i^\star = 0 \tag{32}$$

Without loss of generality, $x_i^\star$ is defined as $Y_i \tilde{y}_i^\star$. Therefore, the above constraint implies that $\tilde{Q}_i \tilde{y}_i^\star = 0$. It can be easily shown that the vector $\tilde{y}_i^\star$ satisfying $\tilde{Q}_i \tilde{y}_i^\star = 0$ is specified as $\tilde{y}_i^\star = \begin{bmatrix} 0 & 0 & \tilde{y}_{3,i}^\star & \tilde{y}_{4,i}^\star \end{bmatrix}^T$. As a result, $x_i^\star = \begin{bmatrix} i_{i,d}^\star & i_{i,q}^\star & I_{i,d}^\star & I_{i,q}^\star \end{bmatrix}^T$ is characterized as follows:

$$\begin{aligned} x_i^\star &= Y_i \tilde{y}_i^\star \\ &= \begin{bmatrix} 0 & 0 & y_{33_i}\tilde{y}_{3,i}^\star + y_{34_i}\tilde{y}_{4,i}^\star & y_{34_i}\tilde{y}_{3,i}^\star + y_{44_i}\tilde{y}_{4,i}^\star \end{bmatrix}^T \end{aligned} \tag{33}$$

Therefore,

$$i_{i,d}^\star = 0 \Rightarrow \dot{i}_{i,d}^\star = 0 \tag{34}$$

$$i_{i,q}^\star = 0 \Rightarrow \dot{i}_{i,q}^\star = 0 \tag{35}$$

and

$$\begin{aligned} I_{i,d}^\star &= y_{33_i}\tilde{y}_{3,i}^\star + y_{34_i}\tilde{y}_{4,i}^\star \\ I_{i,q}^\star &= y_{34_i}\tilde{y}_{3,i}^\star + y_{44_i}\tilde{y}_{4,i}^\star \end{aligned} \tag{36}$$

Considering the system dynamics as well as the conditions in (34) and (35), $u_i^\star = 0$. As a result,

$$\begin{aligned} &K_{P_i}\begin{bmatrix} i_{i,d}^\star \\ i_{i,q}^\star \end{bmatrix} + K_{I_i}\begin{bmatrix} I_{i,d}^\star \\ I_{i,q}^\star \end{bmatrix} = 0 \\ &K_{P_i}\begin{bmatrix} 0 \\ 0 \end{bmatrix} + K_{I_i}\begin{bmatrix} y_{33_i}\tilde{y}_{3,i}^\star + y_{34_i}\tilde{y}_{4,i}^\star \\ y_{34_i}\tilde{y}_{3,i}^\star + y_{44_i}\tilde{y}_{4,i}^\star \end{bmatrix} = 0 \\ &K_{I_i}\begin{bmatrix} y_{33_i} & y_{34_i} \\ y_{34_i} & y_{44_i} \end{bmatrix}\begin{bmatrix} \tilde{y}_{3,i}^\star \\ \tilde{y}_{4,i}^\star \end{bmatrix} = 0 \\ &\begin{bmatrix} g_{13_i} & g_{14_i} \\ g_{23_i} & g_{24_i} \end{bmatrix}\begin{bmatrix} \tilde{y}_{3,i}^\star \\ \tilde{y}_{4,i}^\star \end{bmatrix} = 0 \Rightarrow \begin{bmatrix} \frac{1}{\alpha} & 0 \\ 0 & \frac{1}{\alpha} \end{bmatrix}\begin{bmatrix} \tilde{y}_{3,i}^\star \\ \tilde{y}_{4,i}^\star \end{bmatrix} = 0 \end{aligned} \tag{37}$$

Note that $\begin{bmatrix} g_{13_i} & g_{14_i} \\ g_{23_i} & g_{24_i} \end{bmatrix} = K_{I_i}\begin{bmatrix} y_{33_i} & y_{34_i} \\ y_{34_i} & y_{44_i} \end{bmatrix}$. Based on (37) and (26), $\tilde{y}_{3,i}^\star = 0$ and $\tilde{y}_{4,i}^\star = 0$. Hence, $I_{i,d}^\star = 0$ and $I_{i,q}^\star = 0$. As a result, the largest invariant set of χ is origin and there are not any other system trajectories that converge to the origin. Therefore, the origin of the closed-loop system is asymptotically stable.

4.4 Performance Specifications of Parallel Voltage Source Inverters

One of the requirements of the multivariable current control design in the grid-tied parallel VSIs is that the closed-loop

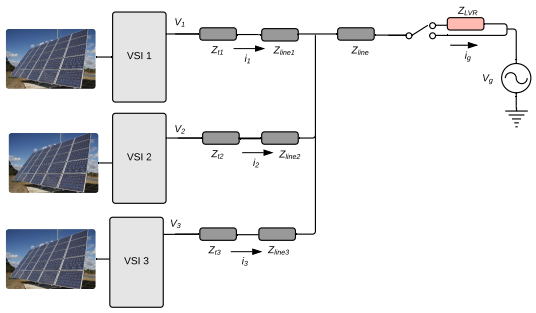

Fig. 4. Schematic diagram of a grid-connected system with 3 VSIs.

response has small rise time and overshoot. Moreover, high closed-loop bandwidth is required to reject low frequency harmonics generated by the grid voltage. The decentralized PI controllers guarantee the stability of the closed-loop parallel VSI system in Fig. 1. However, in order to improve the performance of the closed-loop system, a pre-filter K_{ri} is designed to shape the reference signals. The pre-filter adds a degree of freedom to the control structure. The structure of the two-degree-of-freedom (2DOF) controller is shown in Fig. 3. The pre-filter K_{ri} is designed as a solution of the following optimization problem:

$$\min_{K_{ri}(s)} \quad \left\| T_i(s)K_{ri}(s) - T_{ref,i}(s) \right\|_\infty \tag{38}$$

where $T_i(s)$ is the closed-loop model of VSI i with the PI controller K_i and $T_{ref,i}(s)$ is a reference model designed based on the desired performance of VSI i.

4.5 Proposed Decentralized Vector Current Controller Design Algorithm

The decentralized multivariable vector current controller design for each VSI whose dynamics are given in (10)-(12) is based on the following steps.

Input: Model of each VSI.

Output: Decentralized PI-based vector current controllers K_i and pref-filters K_{ri}.

(i) Finding the decision variables Y_i and G_i via the LMI given in (28).
(ii) Design of the stabilizing PI controllers as $K_i = G_i Y_i^{-1}$.
(iii) Design of the pre-filter K_{ri} using the optimization problem in (38).

5. SIMULATION RESULTS

In this section, we consider a grid-connected system composed of 3 parallel VSIs, as graphically shown in Fig. 4. In order to mitigate over-voltage problems in this grid, an LVR has been installed. Activation of the LVR leads to a drastic increase in the harmonic distortion of the voltage and current signals and a shutdown of all VSIs. As a result, the current controllers of the VSIs must be robust against the change in the grid impedance ($L_g \in \{0, L_{LVR}\}$). The dynamical model and structure of the PLL are given in Equation (9) of Karimi et al. (January 2008).

A. Case Study 1: Current Reference Tracking

The first case study assesses the performance and transient behavior of the proposed current control strategy in current reference tracking. The d and q components of the current signal of VSI1 are initially set at $5A$ and $20A$, respectively. The current reference signals of the d- and q-axis components of the

Table 1. Parameters of parallel inverters in Fig. 4.

L-filter parameters			
		$R_t(m\Omega)$	$L_t(\mu H)$
VSI 1		32	450
VSI 2		32	450
VSI 3		32	450
LVR impedances			
Z_{LVR}		$R_{LVR} = 3m\Omega$	$L_{LVR} = 800\mu H$
Line impedances			
Line 1 impedance	(Z_{line_1})	$r_{line_1} = 0.018\Omega$,	$L_{line_1} = 5.4\mu H$
Line 2 impedance	(Z_{line_2})	$r_{line_2} = 0.018\Omega$,	$L_{line_2} = 5.4\mu H$
Line 3 impedance	(Z_{line_3})	$r_{line_3} = 0.045\Omega$,	$L_{line_3} = 13.5\mu H$
Grid line impedance	(Z_{line})	$R_{line} = 0.252\Omega$,	$L_{line} = 75.6\mu H$
Grid parameters			
$V_g = 230V$			$f_0 = 50Hz$

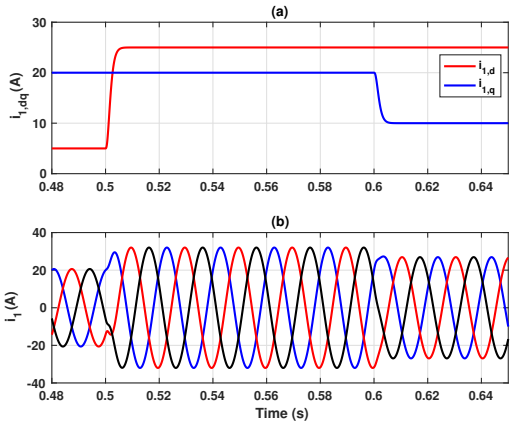

Fig. 5. Dynamic responses of VSI1 due to step changes in reference current signal at $t = 0.5s$ and $t = 0.6s$: (a) dq-components of current signal i_1 and (b) three-phase current i_1.

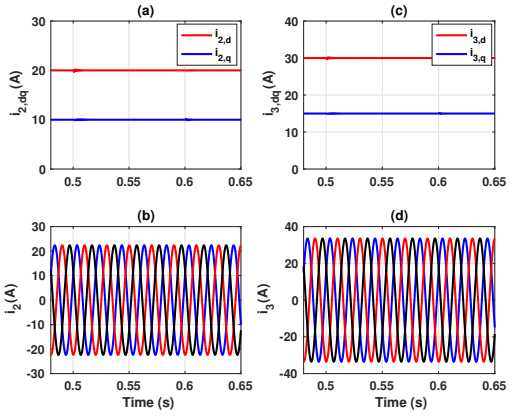

Fig. 6. Dynamic responses of VSI2 and VSI3 due to step changes in reference current of VSI1.

inverter 1 are changed to $25A$ and $10A$ at $t = 0.5s$ and $t = 0.6s$, respectively. Fig. 5 and Fig. 6 respectively show the dynamic responses of VSI1 and other VSIs. The results indicate that the proposed control technique is able to regulate the current signals with zero steady state error, no overshoot, and small transient time (rise time $\leq 2.5ms$). Moreover, the coupling between d and q axes is negligible.

B. Case Study 2: Uncertain Grid Impedance

We study the performance and robustness of the proposed PI-based current controllers against the variations in the grid

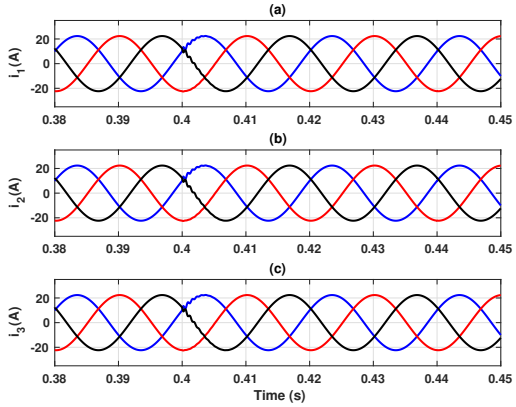

Fig. 7. Dynamic responses of VSIs due to the activation of LVR at $t = 0.4s$.

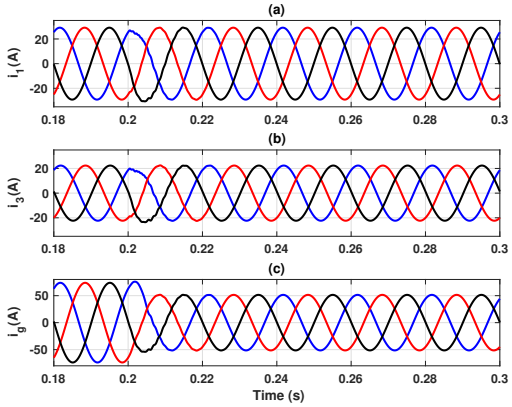

Fig. 8. Three-phase current of VSI1, VSI3, and the grid due to disconnection of VSI2 at $t = 0.2s$.

impedance configuration. To this end, it is assumed that the LVR is initially deactivated. The reference values for $i_{i,d}$ and $i_{i,d}$, $i = 1,2,3$ are respectively set at $20A$ and $10A$. The LVR is suddenly activated at $t = 0.4s$. Fig. 7 shows the three-phase current of all VSIs. As shown, except for some small transients, the change in the grid impedance does not compromise the tracking performance of the proposed current controllers. The results of this test validate the robustness of the proposed active current controller with respect to the grid impedance uncertainty.

C. Case Study 3: Robustness to System Architecture

The main purpose of this case study is to illustrate the superiority of the proposed current controllers in robustness to the uncertainty in the architecture of the parallel voltage source inverters in Fig. 4. To this end, it is assumed that the current controllers regulate the d and q terms of the current of the inverters. The reference values of $i_{i,d}$ and $i_{i,d}$, $i = 2,3$ are respectively set at $20A$ and $10A$ and $i_{1_{ref},d} = 25A$ and $i_{1_{ref},q} = 15A$. At $t = 0.2s$, VSI2 is disconnected from the system. Due to this disconnection, the system architecture is changed. However, since the current controllers are robust with respect to the disconnection of inverters, it does not require to retune the current controller of VSI1 and VSI3. The three-phase current of VSI1 and VSI3 as well as the grid current are depicted in Fig. 8. The results indicate the robustness of the multivariable PI current controllers against uncertainty in the system architecture.

6. CONCLUSION

This paper addresses the problem of scalable design of vector current control of multi-parallel grid-tied voltage source inverters. The control scheme is based on decentralized multivariable PI-based controllers that guarantee stability and track step current references with zero steady-state errors. The proposed current control design strategy is scalable and does not rely on the global model of the whole system. Different case studies of a distribution grid composed of three inverters illustrate the effectiveness of the proposed vector current control technique for multiple grid-connected VSIs. The proposed control approach is also applicable to systems consisting of multiple VSIs with mesh topologies.

REFERENCES

Bahrani, B., Karimi, A., Rey, B., and Rufer, A. (April 2013). Decoupled dq-current control of grid-tied voltage source converters using nonparametric models. *IEEE Trans. on Industrial Electronics*, 60(4), 1356 – 1366.

Bahrani, B., Kenzelmann, S., and Rufer, A. (July 2011). Multivariable-PI-based *dq* current control of voltage source converters with superior axes decoupling capability. *IEEE Trans. Ind. Electron.*, 58(7), 3016–3026.

Bayo-Salas, A., Beerten, J., Rimez, J., and Hertem, D.V. (2016). Analysis of control interactions in multi-infeed VSC HVDC connections. *IET Generation, Transmission & Distribution*, 10, 1336–1344.

Davari, M. and Mohamed, Y.A.R.I. (Feb. 2017). Robust vector control of a very weak-grid-connected voltage-source converter considering the phase-locked loop dynamics. *IEEE Trans. on Power Electronics*, 32(2), 977–994.

Hannan, M.A., Hussin, I., Ker, P.J., Hoque, M.M., Lipu, M.S.H., Hussain, A., Rahman, M.S.A., Faizal, C.W.M., and Blaabjerg, F. (December 2018). Advanced control strategies of VSC based HVDC transmission system: Issues and potential recommendations. *IEEE Access*, 6, 78352–78369.

Kammer, C., D'Arco, S., Endegnanew, A.G., and Karimi, A. (Jul. 2019). Convex optimization-based control design for parallel grid-connected inverters. *IEEE Trans. on Power Electronics*, 34(7), 6048–6061.

Karimi, H., Yazdani, A., and Iravani, R. (January 2008). Negative-sequence current injection for fast islanding detection of a distributed resource unit. *IEEE Trans. Power Electron.*, 23(1), 298–307.

Khalil, H.K. (2006). *Nonlinear Systems*. Prentice Hall, New Jersey.

Li, G.J., Ruan, S.Y., Ooi, B.T., Sun, Y.Z., and Choi, S.S. (2010). Autonomous AC grid based on multi-infeed voltage source converter stations. *Electric Power Components and Systems*, 38, 558–574.

Sadabadi, M.S., Haddadi, A., Karimi, H., and Karimi, A. (Oct. 2017). A robust active damping control strategy for an LCL-based grid-connected DG unit. *IEEE Trans. Ind. Electron.*, 64(10), 8055–8065.

Schauder, C. and Mehta, H. (1993). Vector analysis and control of advanced static VAR compensators. In *IEE Proceedings C, Generation, Transmission and Distribution*, volume 140, 299–306.

Svensson, J. (May 2001). Synchronisation methods for grid-connected voltage source converters. *IET Proceedings - Generation, Transmission and Distribution*, 148(3), 229–235.